J. COMBIN. MATH. COMBIN. COMPUT. 127a (2025) 9099--9115

Journal of Combinatorial Mathematics and Combinatorial Computing
www.combinatorialpress.com/jcmcc

Combinatorial Press

Simulation analysis of external characteristics of medium voltage flexible interconnection system and research on protection control strategy

Shijin Xin[1,✉], Kan Feng[2], Guojie Hao[3], Xiaofeng Wang[4], Qing Xu[3], Libao Wei[3]

[1] Energy Development Research Center, Baiyin Power Supply Company, Baiyin, Gansu, 730900, China
[2] Party Committee, Baiyin Power Supply Company, Baiyin, Gansu, 730900, China
[3] Development Planning Department, Baiyin Power Supply Company, Baiyin, Gansu, 730900, China
[4] Dispatching Center, Baiyin Power Supply Company, Baiyin, Gansu, 730900, China

ABSTRACT

The article preliminarily studies the structure of flexible interconnection system of MV distribution network, and understands the application scenario and equipment composition of the flexible system. For the purpose of reducing SOP loss, transformer loss and line loss, the operation of the MV flexible interconnected distribution network is optimized, the operation optimization model of the flexible interconnected distribution network is constructed, and the fault enumeration method is adopted as the reliability assessment method of the flexible interconnected system. Through experimental simulation, the stability, reliability and dynamic characteristics of the MV flexible interconnection system are explored respectively, and the system protection control strategy is proposed. For the same constant power load step, the larger the voltage loop proportional parameter is, the more stable the system tends to be, and the larger the voltage loop integral parameter and the station circuit parameter are, the more unstable the system tends to be. The maximum mutation value of the system constant power load gradually decreases when the station load power gradually increases. The reliability of the MV flexible interconnection system increases with the increase of SOP capacity. In the medium voltage flexible distribution interconnection system. The system damping, oscillation frequency and overshoot are significantly reduced and the peak time is increased when the DC voltage sag factor is increased.

Keywords: flexible interconnection, medium voltage distribution network, SOP, characterization simulation, protection control

✉ Corresponding author.
E-mail address: w18032636560@yeah.net (S. Xin).
Received 25 March 2024; Revised 05 June 2024; Accepted 15 December 2024; Published Online 15 April 2025.
DOI: 10.61091/jcmcc127a-506

1. Introduction

Most distribution networks adopt "closed-loop design and open-loop operation", using contact switches to form hand-in-hand or mesh distribution networks in each sub-district to realize sectional control and post-accident load transfer. However, there are problems associated with this model. First, due to the rapid growth and unbalanced development of loads, the medium voltage distribution network in the load center city has the problems of tense distribution corridors, high feeder loading rate and unbalanced distribution [1-2]. Second, when distribution network faults occur, load transfer is usually carried out by closing contact switches, which, once improperly operated, may lead to power supply interruptions and ring-closing shocks, and expand the scope of faults [3-4]. Thirdly, the access of new sensitive DC loads puts higher requirements on power supply reliability, while the open-loop operation method can lead to short-term outages in non-faulted areas, limiting the improvement of power supply reliability [5-7]. Meanwhile, the promotion of the application of renewable energy and energy storage at the policy level makes the MV distribution system face problems such as trend reversal and complex operation mode, and the ability of open-loop operation and trend regulation is further limited [8-10].

In order to better adapt to wind power, photovoltaic power generation and other distributed power sources, as well as energy storage devices, electric vehicles and other broad load access to a large number of medium-voltage interconnection distribution system as the core of the flexible interconnection device has been widely concerned by academics and the engineering community. The basic concept is to rely on back-to-back voltage source converters to realize the interconnection of distribution network feeders, thus realizing the closed-loop operation of the distribution network and optimizing the distribution of currents, and improving the flexibility of grid control and reliability of power supply [11-14]. By controlling the current in the DC link, power equalization between different AC divisions can be accomplished without considering the frequency synchronization problem [15-16]. Compared with distribution network sectionalized and contact switches, FID technology is easier to realize fault isolation, which greatly improves the flexibility and safety of distribution network control [17-18]. When FID technology is used for MV feeder interconnection, asynchronous loop operation between multiple AC distribution feeders can be accomplished without increasing the short-circuit capacity, which can play the roles of trend transfer, load ratio balancing, network loss reduction, fault isolation, and power supply restoration, etc., and realize the multi-terminal loop operation between feeders and the optimal allocation of adjustable resources [19-22].

In this paper, based on the application scenarios and constituent equipment of the flexible interconnection system of the MV distribution network, the traditional MV flexible interconnection system is optimized in order to reduce the SOP losses, transformer losses, and line losses. Reliability assessment of the flexible interconnected distribution network is carried out by fault enumeration method. Simulation experiments are utilized to study the effects of control parameters, station load power allocation and circuit parameters on system stability, the effects of SOP capacity on system reliability, and to explore the dynamic characteristics of the flexible interconnection system of MV distribution grids using DC voltage as an example. Finally, the control and protection strategies in the flexible interconnection system of MV distribution grid are studied in depth, and the system control scheme and protection configuration are designed.

2. Medium-voltage distribution network flexible interconnection system

2.1. Structure of the flexible interconnection system for MV distribution grids

2.1.1. Application scenarios. Flexible interconnection equipment is a kind of equipment based on modern power electronic technology, installed in the distribution network, used to connect two or more distribution feeders, through active/reactive power control at the feeder level, regulating and optimizing the distribution of the current at the system level, and then integrating all kinds of dispatchable source and load resources in the distribution system, and ultimately realizing the enhancement of the overall operation level of the system [23]. The difference between flexible interconnection equipment and flexible AC transmission systems (FACTS) such as controllable series compensation devices (TCSC), static synchronous series compensators (SSSC) and unified current controllers (UPFC) lies in the fact that flexible interconnection equipment is required to have the ability of trend regulation and fault isolation at the same time. Flexible interconnection equipment, as an important support for the flexible characteristics of distribution networks, is narrowly defined as multiport power electronic equipment that realizes flexible interconnection of multiple AC feeders, represented by back-to-back voltage source converters, while broadly defined flexible interconnection equipment is rich in various forms, including power electronic transformers, energy routers, soft-contact switches, and intelligent power/information switching base stations.

There are usually two application scenarios for flexible interconnection in MV distribution networks as shown in Figure 1. Scenario 1: Connecting multiple feeders from the same substation. According to the siting and capacity planning, the flexible interconnection equipment can be installed at the end of the feeder or other preferred locations to regulate the currents between different feeders of the same substation and optimize the current distribution. Scenario 2: Connecting multiple feeders from different substations to achieve combined loop operation of distribution networks with different voltage levels and phases for wider trend optimization. In Scenario 1 and Scenario 2, while connecting two or more AC feeders, the flexible interconnection equipment can provide DC interfaces for DC distribution lines as well as DC equipment such as new energy power generation, energy storage and charging piles, forming a hybrid AC-DC flexible interconnection under reasonable system design.

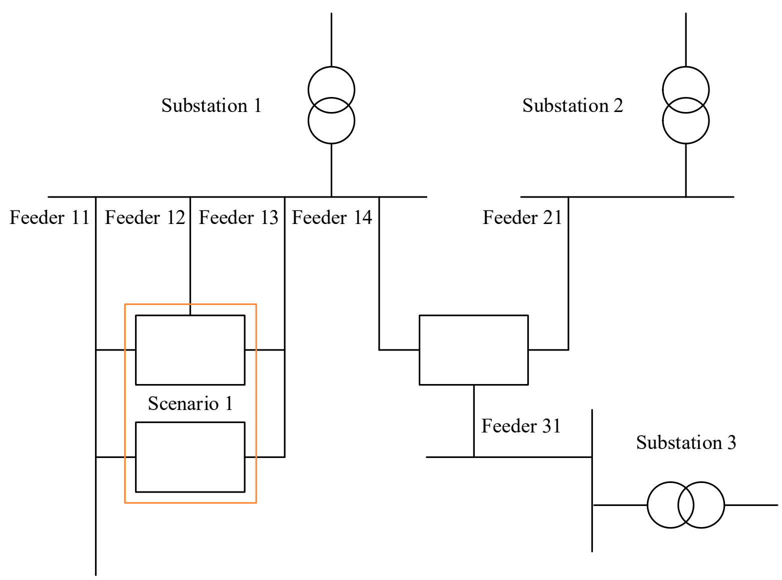

Fig. 1. Form of flexible interconnection of medium-voltage distribution network

2.1.2. Composition of equipment. From a functional point of view, the flexible interconnection equipment is an important node for energy redistribution in the distribution network, which needs to have both power and information monitoring and processing functions. Therefore, the flexible interconnection equipment usually consists of two parts: the cooperative controller and the power converter, and the basic composition of the flexible interconnection equipment is shown in Figure 2.

The main function of the cooperative controller is to centrally manage and optimize the energy of the AC feeder and DC equipment connected to the flexible interconnection equipment according to the operation commands of the upper control system such as the distribution automation system, combined with the collected operation data of the AC feeder and DC line/equipment [24-25]. The time scale of the co-controller is in the order of seconds, and the main control strategies include power/energy allocation to individual ports, feeder voltage regulation, and multi-operation mode switching.

The power converter realizes the power conversion according to the commands of the co-controller to achieve the set target of power/energy allocation. The power converter usually consists of a current converter module, a control module, an AC interface and a DC interface module. Among them, the converter module mainly includes AC/DC converter, DC/DC converter and other power conversion circuits. The control module mainly refers to the control of power conversion circuits, usually in the form of embedded controllers, including sampling and rectification, digital arithmetic, modulation output and other links. The control module designs closed-loop control based on the received reference voltage or power command, relying on the gathered in situ information. The control module is required to achieve power balance between multiple ports, which is the basis for safe and stable operation of flexible interconnected devices. The time scale of the control module is within a hundred milliseconds, and the main control strategies include DC bus voltage control, flexible interconnection power control and AC feeder voltage control, and multiple operation mode switching.

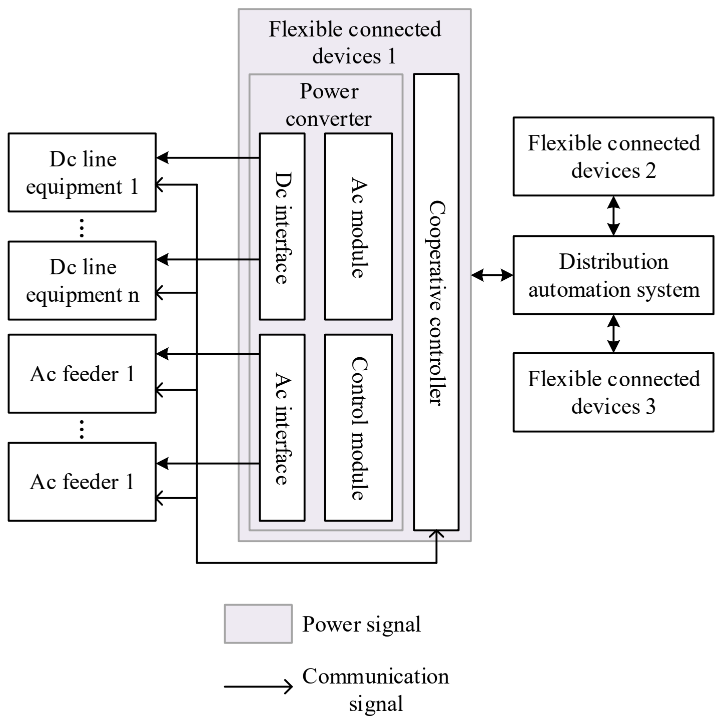

Fig. 2. Basic composition of flexible interconnection device

2.2. *Flexible Interconnection Distribution Grid Operation Optimization Model*

In this paper, the operation optimization is aimed at reducing the comprehensive loss of the system, and the loss of the flexible interconnection system consists of three parts: SOP loss, transformer loss, and line loss. Therefore, the objective function is set up as:

$$\min F = \min(F_1 + F_2 + F_3) \tag{1}$$

where, F is the integrated system loss, F_1 is the SOP power transmission loss, F_2 is the transformer loss, and F_3 is the network line loss.

1) SOP loss calculation. SOP loss of each port is independent of each other, its loss is mainly related to the port transmission power and its transmission efficiency, the formula is:

$$F_1 = \sum_{n=1,2,3} (1-\eta_{sn}) S_{sn} \tag{2}$$

where $S_s n$ is the transmitted power of SOP port n and η_{sn} is the power transfer efficiency of port n.

The three-port SOP needs to satisfy the active power conservation constraint. If the SOP power transmission direction is taken as the positive direction, we have:

$$P_{s1} + P_{s2} + P_{s3} = 0 \tag{3}$$

In addition, the SOP needs to consider the port capacity constraint, i.e., the transmission power S_{sn} of the SOP port should be less than its own capacity S_{sop}, there:

$$S_{sn} \le S_{sop} \tag{4}$$

2) Transformer loss calculation. In this paper, the two transformer losses can be expressed as:

$$F_2 = \sum_{m=1,2} P_{bm,loss} \tag{5}$$

where, $P_{bm,loss}$ is the loss of transformer T_m.

Based on the transformer loss characterization, the best economic operation interval operation constraint is established, i.e.:

$$0.16 \le \beta_m \le 0.75 \tag{6}$$

where β_m is the load factor of transformer T_m.

In addition, the transformer also needs to satisfy the capacity constraints with:

$$S_{bm} = \sqrt{P_{bm}^2 + Q_{bm}^2} \le S_{rm} \tag{7}$$

where S_{bm} is the actual apparent power transmitted by transformer T_m and S_{rm} is the capacity of transformer T_m.

3) Network line loss calculation. The network line loss is modeled based on the branch current model, and the network line loss calculation formula is:

$$F_3 = \sum I_{ij}^2 r_{ij} \tag{8}$$

where I_{ij} is the ij-branch current.

The operation constraints contain network operation safety constraints and network current constraints. The network operation safety constraint can be expressed as:

$$\begin{cases} V_{i,\min} \le |V_i| \le V_{i,\max} & \forall i \in N_{\text{bus}} \\ s_{i,\min} \le |s_i| \le s_{i,\max} & \forall i \in N_{\text{bus}} \\ |I_{ij}| \le I_{ij,\max} & \forall (i,j) \in N_{\text{brand}} \end{cases} \tag{9}$$

where V_i is the node voltage, $V_{i,\max}$ and $V_{i,\min}$ are its upper and lower limits, respectively, $s_{i,\max}$ and $s_{i,\min}$ are the upper and lower limits of the node power s_i, respectively; and $I_{ij,\max}$ is the upper limit of the branch current I_{ij} mode value.

The network current constraint is a non-convex constraint, which is relaxed in two steps in this paper to improve the solution rate. Order $\tilde{I}_{ij} = |I_{ij}|^2, \tilde{V}_i = |V_i|^2$, the final network current constraint can be expressed as follows:

$$\begin{cases} p_j = \sum_{k,j-k} P_{jk} - \sum_{i,i-j} (P_{ij} - \tilde{I}_{ij} r_{ij}) \\ q_j = \sum_{k,j-k} Q_{jk} - \sum_{i,i-j} (Q_{ij} - \tilde{I}_{ij} x_{ij}) \quad \forall j \in N_{bas} \\ \tilde{V}_i = \tilde{V}_j - 2(r_{ij} P_{ij} + x_{ij} Q_{ij}) + (r_{ij}^2 + x_{ij}^2) \tilde{I}_{ij} \\ \tilde{I}_{ij} \geq \frac{P_{ij}^2 + Q_{ij}^2}{\tilde{V}_i} \quad \forall (i,j) \in N_{branch} \end{cases} \tag{10}$$

2.3. Independent Reliability Assessment Methodology for Flexible Interconnections

The fault enumeration method is used to assess the reliability of flexible interconnected distribution networks. Firstly, the fault scenarios of the distribution network are enumerated, then the influence range of the faults is analyzed, and finally, all the fault scenarios are integrated to obtain the reliability indexes of individual customer load nodes and the overall power supply of the distribution network.

In the case of a flexible interconnected distribution network, the SOP equipment inside the network can restore the power supply to the loads that were disconnected at the initial moment of the fault by means of fault reconfiguration in the event of a fault in a component of the distribution network. The loads affected by the fault can be categorized into short-term interrupted loads (corresponding to the operating time required for the actuators of the flexible interconnected distribution network to operate in order to realize the fault reconfiguration t_{r}) and long-term interrupted loads (corresponding to the restoration time of the faulted components t_{f}).

In order to fully utilize the fault load transfer capability of the SOP to minimize the long-time power supply interruption load, when the SOP participates in the fault reconfiguration of the distribution network, it adopts the operation mode of maximum reactive power output in order to raise the voltage magnitude of the end of the feeder as much as possible, so as to maximize the scope of the fault load transfer.The calculation of the reactive output of the SOP is shown in Eq. (11), and its reactive output is taken as a known condition to carry out the post-fault distribution network trend Calculation:

$$Q_{SOP} = \sqrt{S_{SOP}^2 - (P_{L,pre} - P_{L,pos})^2} \tag{11}$$

where Q_{sop} is the reactive power output from the SOP to the feeder where load transfer is performed, S_{sop} is the rated capacity of the SOP, $P_{L,pre}$ is the amount of lost load of the distribution network before fault reconfiguration. That is, the sum of short-time and long-time power supply interruption loads, $P_{L,pos}$ is the loss of load of the distribution network after the fault reconfiguration, i.e., the long-time power supply interruption load, and $P_{L,pre} - P_{L,pos}$ corresponds to the size of the active load transferred.

3. Characterization simulation analysis

3.1. Stability analysis

In order to verify the stability of the flexible interconnection system of MV distribution grid in this paper, hardware-in-the-loop experiments are conducted using RTLAB and TMS320f28377d microprocessor.

3.1.1. Effect of control parameters on stability. Only the effect of sudden change of constant power load on the system is considered, i.e., the system satisfies the necessary conditions such as small signal stabilization and power balance. Consider the constant power load from 50kW to 150kW. 4 different sets of voltage loop PI parameters are selected, and the experimental results under different control parameters are shown in Fig. 3, from top to bottom are serial numbers 1 to 4, where v_{dc} is the DC bus voltage. Under the control parameters of No. 1 and No. 4, when the constant power load is changed from 50kW to 150kW, the DC bus voltage starts to oscillate, and the system is destabilized and cannot reach the equilibrium point. The system is able to cope with the sudden change in the constant power load under the parameters of serial number 2 and serial number 3. For the same constant power load step, the larger the voltage loop proportional parameter k_{pv} is, the system tends to stabilize, and the larger the voltage loop integral parameter k_{iv} is, the system tends to destabilize, and the application of this criterion can guide the direction of system control parameter modification.

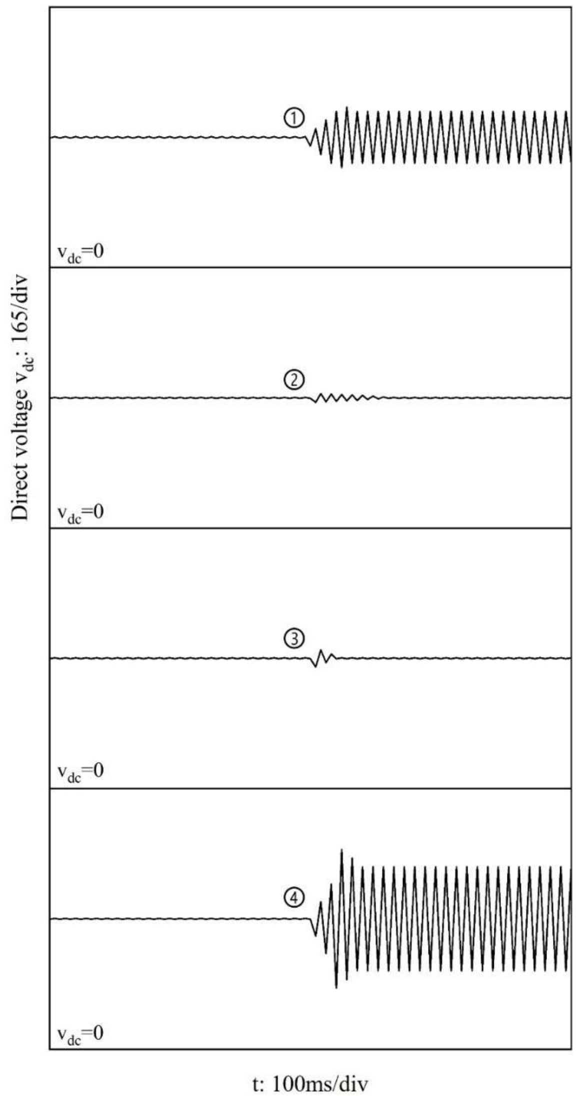

Fig. 3. Experimental results under different control parameters

3.1.2. Effect of circuit parameters on stability. Hardware-in-the-loop experimental verification of the circuit parameters is carried out, four sets of circuit parameters are selected, and the constant power load on the DC bus is stepped from 50kW to 150kW, and the experimental results are shown in Fig. 4. The results show that the larger the station circuit parameters are, the more unstable the system tends to be when sequence numbers 1, 2 and 3 face the same constant power load mutation. However, the DC bus voltage tends to stabilize after a period of oscillation under the parameter of serial number 4. Continuing to increase the table area circuit parameter R_f so that R_f =0.5Ω and other parameters remain unchanged, the system destabilizes when the constant power load is suddenly changed.

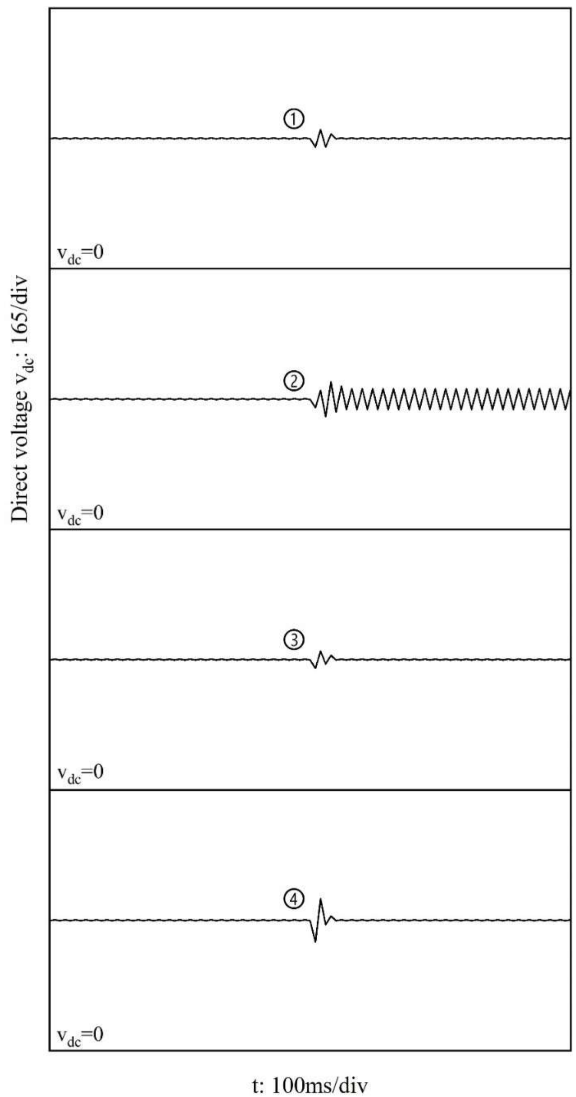

Fig. 4. Experimental results under different circuit parameters

3.1.3. Impact of station load power distribution on stability. When the system faces a perturbation in the lower left region, it can be determined that the system can definitely be stabilized to a new equilibrium point, and when facing a perturbation in the upper right region, the system is not necessarily destabilized. Hardware-in-the-loop experiments are carried out on the load power of the station for 2 operating conditions and stability prediction. The experimental results under different AC loads are shown in Fig. 5. The results show that as the station load power increases, the maximum mutation value of constant power load that the system can withstand gradually decreases, and when the station load power is 100kW, the constant power load on the DC bus mutates to 150kW, and the DC bus voltage oscillates and gradually destabilizes, and the experimental results are consistent with the predicted results of the stability criterion.

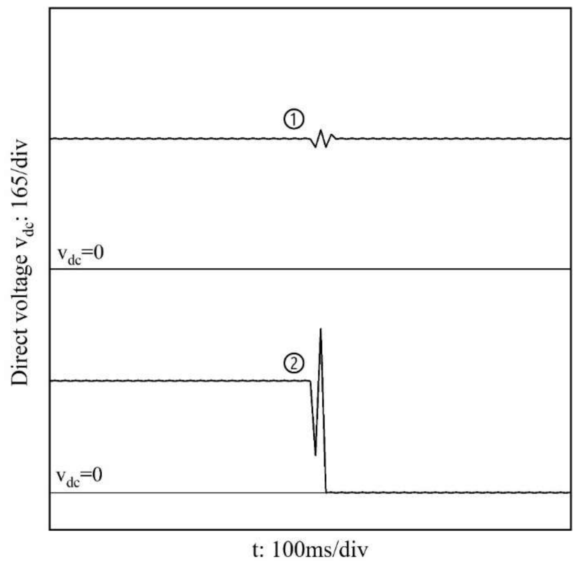

Fig. 5. Experimental results under different AC loads

3.2. Reliability analysis

3.2.1. Analysis of SOP's Rapid Supply Transfer Strategy. The reliability assessment results of FIDN (Flexible Interconnected Distribution Network) under different fast transfer strategies (S1, S2, S2') of SOP are shown in Table 1 (Reliability metrics are selected as system average outage frequency ISAIFI, system average outage duration ISAIDI, system average power supply reliability IASAI, and system shortage of power supply IEENS).

From the table, it can be seen that the FIDN system reliability metrics under strategies S2 and S2' are better than those of strategy S1, which is due to the fact that strategies S2 and S2' take into account the SOP short-term overload capability, while strategy S1 performs fast transfer of supply only when the SOP capacity is larger than the transfer resupply load. In addition, compared to strategy S2, the system reliability index under strategy S2' is further improved because strategy S2' performs fast transfer under any fault scenario and determines the restoration of the transfer load based on the SOP maximum overload operation time and the SOP overload elimination time.

Table 1. System reliability indices under different transfer strategies for SOP

System reliability index	S1	S2	S2'
I_{SAIFI} (time/a)	2.103	2.103	2.103
I_{SAIDI} (h/a)	2.442	2.428	2.422
I_{ASAI} (%)	99.988	99.988	99.988
I_{EENS} (MWh/a)	26.845	26.672	26.523

The SOP fast transfer of supply under the three strategies is shown in Fig. 6 (where a vertical coordinate of 1 indicates that the SOP fast transfer of supply after fault isolation, and vice versa is 0). Fig. 6 further shows that the number of SOP fast turn-ons under strategies S1, S2, and S2' increases sequentially due to the consideration of SOP short-time overload capability. For the convenience of analysis and to fully utilize the enhancement of SOPs on FIDN reliability, strategy S2' is adopted in all the following scenarios.

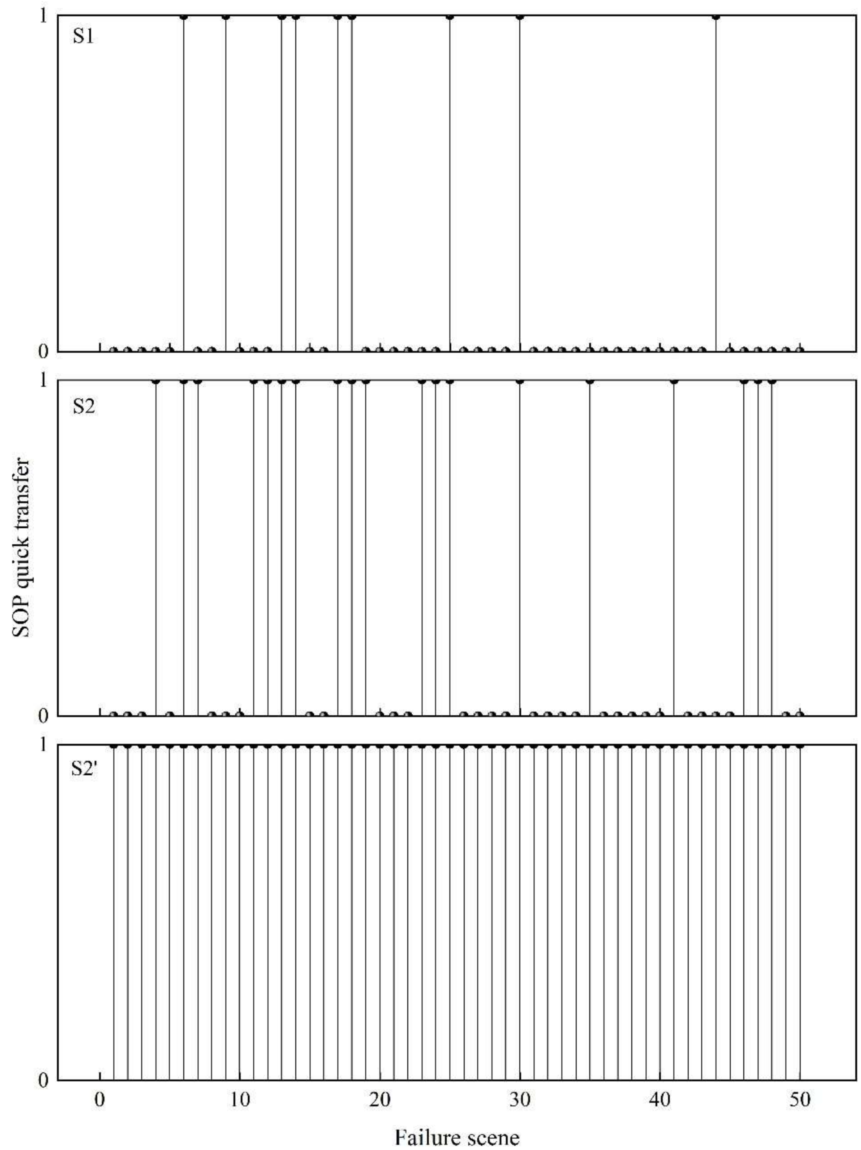

Fig. 6. SOP fast transfer situation under three strategies

3.2.2. Impact Analysis of SOP Capacity on FIDN Reliability. The SOP capacity is set to 60%, 80%, 100%, 120%, 140%, 160%, 180%, and 200% of the original (4 MVA) to analyze the impact of the change of SOP capacity on the reliability of FIDN. The variation of FIDN reliability under different SOP capacities is shown in Fig. 7 (where Scenario 1 is the “closed-loop design, open-loop operation” distribution network).

As can be seen in Fig. 7, the FIDN reliability continues to increase as the SOP capacity continues to increase (I_{ASAI} continues to increase and I_{SAIDI} continues to decrease). When the SOP capacity is 4MVA, although the power outage time of some load points in FIDN is basically equivalent to the distribution network of "closed-loop design and open-loop operation", considering the effect of SOP rapid transfer on the power outage time of other load points, on the whole (as shown in Figure 7), the improvement of the reliability of FIDN by SOP fast transfer has basically completely offset the negative impact of the reliability caused by the expansion of the fault set. When the SOP capacity is increased to 8 MVA, the FIDN reliability will no longer change, i.e., the SOP capacity of 8 MVA basically meets the requirement of rapid load transfer under various fault scenarios.

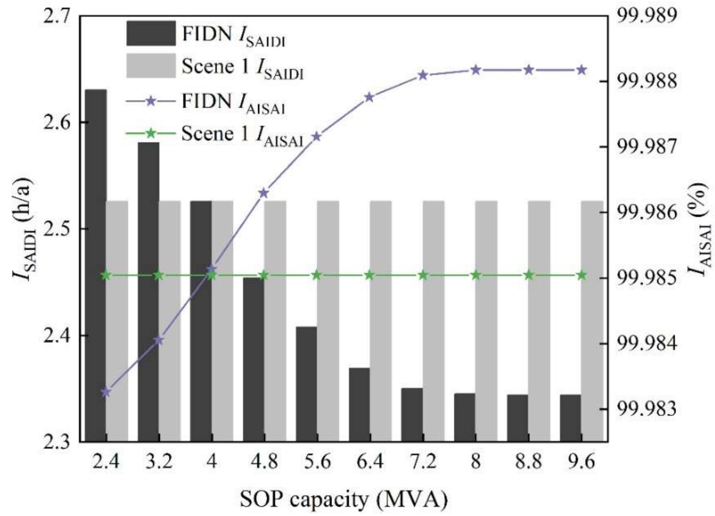

Fig. 7. Variation of FIDN reliability with different SOP capacities

3.3. Dynamic characterization

In this section, the dynamic characteristics of the MV flexible interconnected distribution network system are analyzed using the DC voltage as an example.

The effects of the sag coefficient (R_d) of the current sag control system on the dynamic characteristic indexes of the dc bus voltage are shown in Fig. 8, with (a) and (b) showing the effects of the sag coefficient (R_d) on the damping coefficient (ζ) and the oscillation frequency (ω_d), and the effects of the sag coefficient (R_d) on the peak time (t_p) and the overshooting amount (σ), respectively.

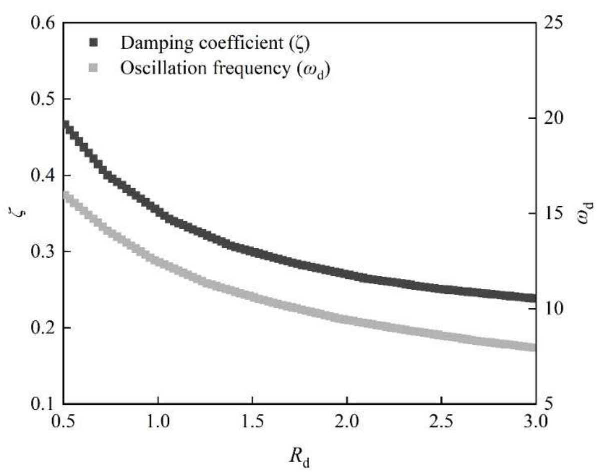

(a) Damping coefficient (ζ) and oscillation frequency (ω_d)

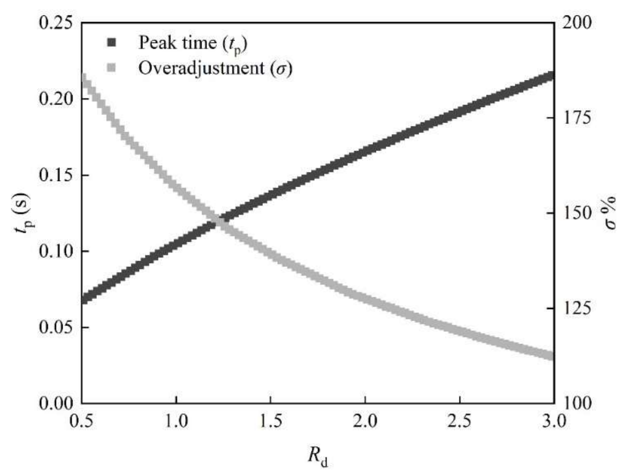

(b) Peak time (t_p) and overadjustment (σ)

Fig. 8. The effect of drooping coefficient on dynamic characteristics of the system

The dynamic response of the DC bus voltage when the sag coefficient changes is shown in Fig. 9, and the load resistance R_{load} is reduced from 200 Ω to 100 Ω at the 4th second in order to simulate the constant power load perturbation, and the results of the calculation of the corresponding dynamic characteristic indexes are shown in Table 2. From Fig. 9 and Table 2, it can be seen that in this paper, the DC voltage dynamics of the medium voltage flexible distribution network interconnection system, the sag coefficient increases, the system damping, oscillation frequency and overshooting are significantly reduced, and the peak time increases. When the sag coefficient R_d is increased from 0.5 pu to 1.5 pu, the system damping ζ, oscillation frequency ω_d and overshooting amount σ are reduced by 0.168, 5.37 rad/s and 47%, respectively, and the peak time is increased by 0.069s.

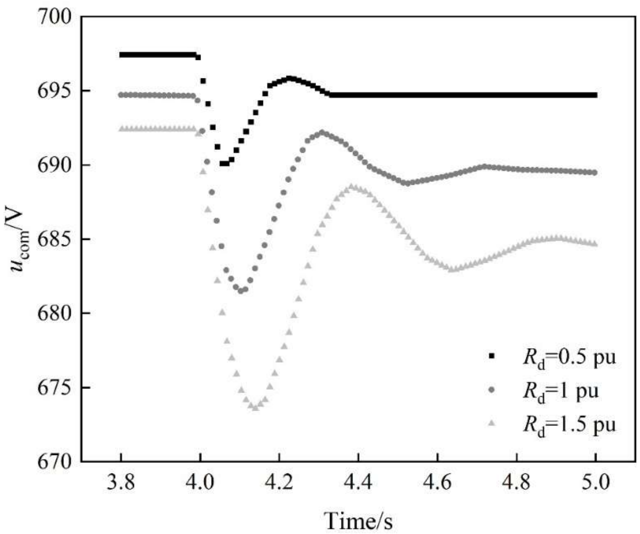

Fig. 9. The direct current voltage dynamic response in the change of drooping coefficient

Table 2. The dynamic characteristics calculation results in the change of drooping coefficient

Mode	Index	R_d=0.5 pu	R_d=1 pu	R_d=1.5 pu
Current drooping control	ζ	0.467	0.351	0.299
	ω_d (rad/s)	15.96	12.43	10.59
	t_p (s)	0.068	0.105	0.137
	σ %	186	156	139

4. System control and protection strategy

4.1. System Control Program

According to the scope of action and function division, the control system is divided into three levels: dispatching control layer, coordination control layer and local control layer. The dispatching control layer is the top-level external control, which determines the operation mode of the flexible interconnection system according to the dispatching demand of the main station of the distribution network and gives the corresponding reference instruction. Coordination control layer is the centralized control of the upper layer, which controls the coordinated work of each key equipment according to the operation mode and reference instruction given by the upper layer, and realizes smooth switching of the system operation mode and coordinated response in case of AC failure. The local control layer is the decentralized control of the lower layer, which is controlled by the modular multilevel converter (MMC), DC transformer (DCT) and other key devices according to their own principles and characteristics to realize the control requirements given by the upper layer. The block diagram of the control system of the demonstration project is shown in Figure 10.

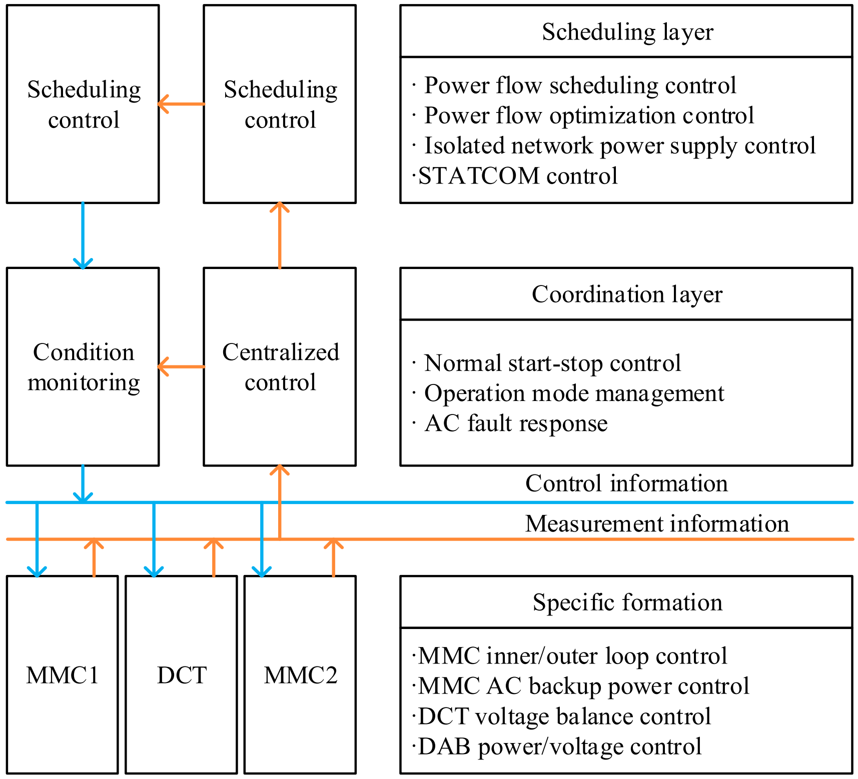

Fig. 10. Control system block diagram of the demonstration project

Among other things, the STATCOM control utilizes the reactive power control capability of the MMC to provide static reactive power compensation (STATCOM) functionality to the grid.

In the coordination and control layer, there are mainly five operation modes in the flex-direct interconnection system, namely, shutdown, one-side shutdown, STATCOM operation, back-to-back operation, and AC standby power operation, and the conversion relationship between the operation modes is shown in Fig. 11. Among them, normal startup, normal shutdown, operation mode management, and AC fault response are the main control functions of the coordination control layer. Normal startup and shutdown control specifies the switching strategy between the shutdown mode and other operation modes of the flex-straight interconnection system, including the normal startup control and normal shutdown control of the STATCOM operation mode and one-side shutdown mode. The operation mode management specifies the switching strategy of the other four operation modes of the flexible interconnected system except the shutdown mode in the normal working state, which is the main coordinating control function to interface with all kinds of control commands of the dispatching control layer. AC fault response is only activated when the system is in back-to-back operation mode, which stipulates how to locate the fault location and make different responses according to the fault location when AC fault is detected by the flexible interconnection system in back-to-back operation mode, so as to quickly restore power supply to non-faulty areas.

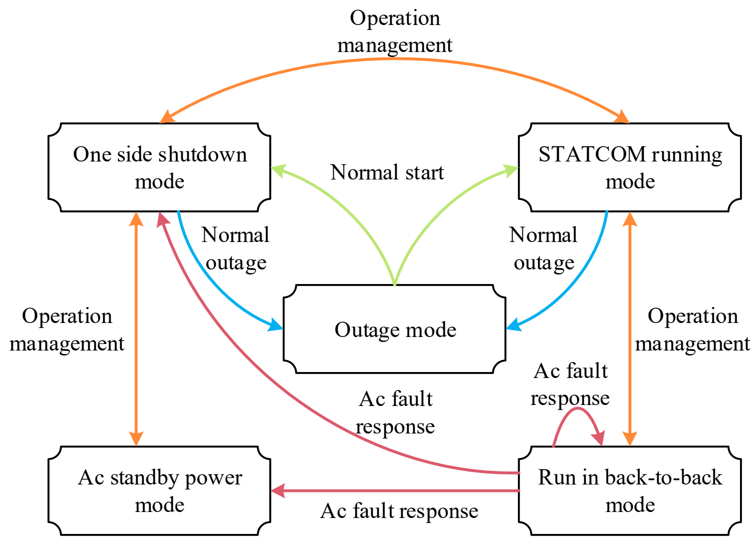

Fig. 11. Transition relationship of system operation modes

4.2. System protection configuration

Due to the lower voltage level of 10kV MV distribution field and the higher requirements for equipment compactness and simplification, the demonstration project adopts the secondary design principle of control and protection integration, and the relay protection of the flexible direct interconnection system is independently configured by each key equipment in the system and deployed in combination with its control equipment at the local control layer. The protection function configuration of MMC and DCT in the system is shown in Fig. 12 and Fig. 13 respectively. Among them, each key device takes its own working range as the protection area, and the protection areas of each key device overlap with each other, so as to ensure reliable protection for all faults within the system.

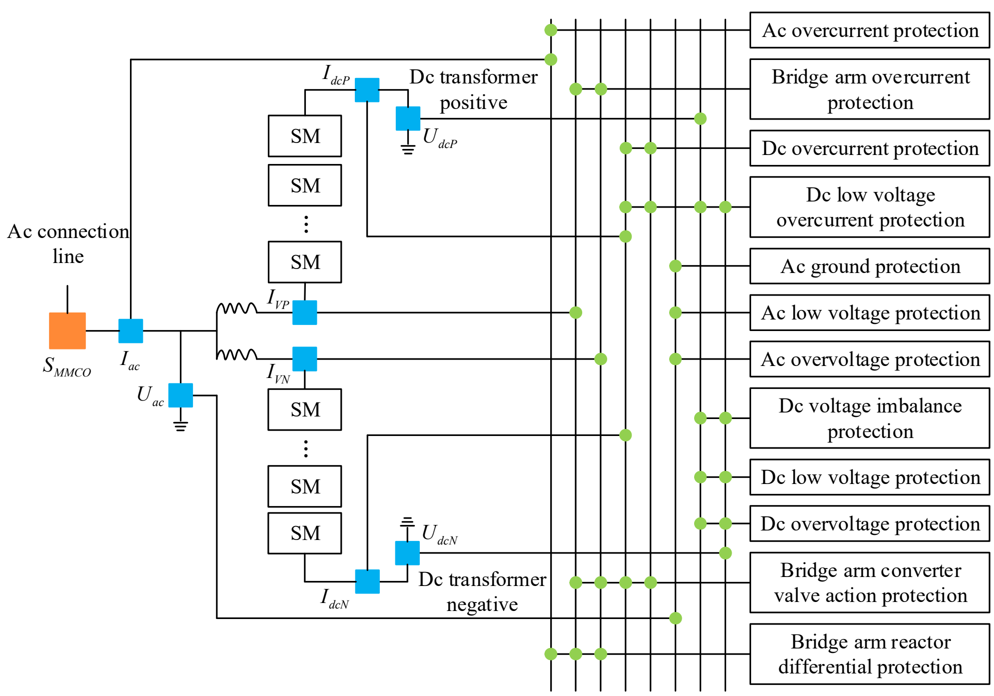

Fig. 12. Relaying protection functions of MMC

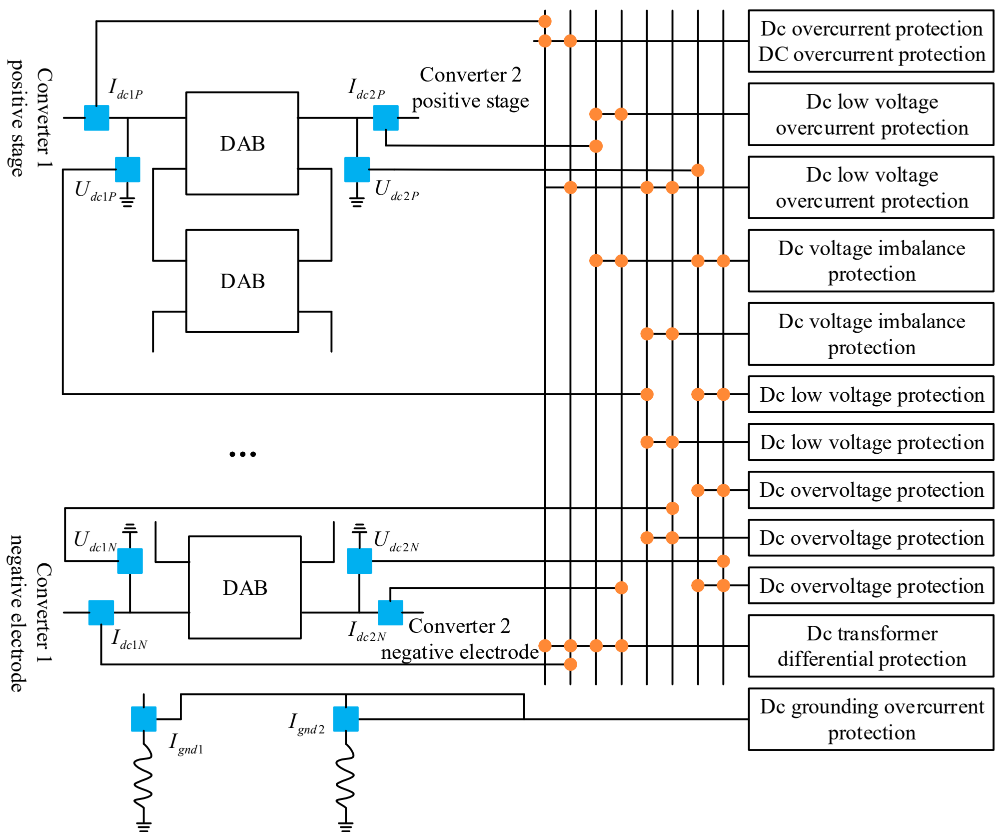

Fig. 13. Relaying protection functions of DCT

5. Conclusion

This paper analyzes the application scenarios and equipment composition of the flexible interconnection system of MV distribution network, and optimizes the operation of the flexible interconnection distribution network, and explores the reliability assessment method of the flexible interconnection system. Through simulation experiments, the stability, reliability and dynamic characteristics of the MV flexible interconnection system are analyzed, and the system control and protection strategies are studied.

1) For the same constant power load step, the larger the voltage loop proportional parameter k_{pv}, the more stable the system tends to be, and the larger the voltage loop integral parameter k_{iv}, the more unstable the system tends to be. For the same constant power load step, the larger the station circuit parameter, the more unstable the system tends to be. The maximum constant power load mutation value that the system can withstand decreases gradually with the increase of the station load power.

2) The system reliability index under strategy S2' is better than that of S1 and S2. The reliability of the medium voltage flexible interconnection system continues to improve as the SOP capacity continues to increase.

3) In the medium-voltage flexible distribution interconnection system. When the DC voltage sag coefficient R_d is increased from 0.5 pu to 1.5 pu, the system damping ζ decreases from 0.467 to 0.299, the oscillation frequency ω_d decreases from 15.96 rad/s to 10.59 rad/s, the overshooting amount σ decreases from 186% to 139%, and the peak time increases from 0.068 to 0.137s.

Funding

This project is funded by the Gansu Electric Power Company Science and Technology Project of State

Grid in 2024: Research on key Technology and typical configuration of flexible interconnection of Medium voltage Distribution Network (No.: B72703241203).

References

[1] Peng, F. Z. (2017). Flexible AC transmission systems (FACTS) and resilient AC distribution systems (RACDS) in smart grid. Proceedings of the IEEE, 105(11), 2099-2115.

[2] Wu, P., Huang, W., Tai, N., & Liang, S. (2018). A novel design of architecture and control for multiple microgrids with hybrid AC/DC connection. Applied Energy, 210, 1002-1016.

[3] Ji, H., Wang, C., Li, P., Ding, F., & Wu, J. (2018). Robust operation of soft open points in active distribution networks with high penetration of photovoltaic integration. IEEE Transactions on Sustainable Energy, 10(1), 280-289.

[4] Ji, H., Wang, C., Li, P., Zhao, J., Song, G., Ding, F., & Wu, J. (2017). An enhanced SOCP-based method for feeder load balancing using the multi-terminal soft open point in active distribution networks. Applied Energy, 208, 986-995.

[5] Agcayazi, T., Chatterjee, K., Bozkurt, A., & Ghosh, T. K. (2018). Flexible interconnects for electronic textiles. Advanced Materials Technologies, 3(10), 1700277.

[6] Islam, M. R., Mahfuz-Ur-Rahman, A. M., Muttaqi, K. M., & Sutanto, D. (2018). State-of-the-art of the medium-voltage power converter technologies for grid integration of solar photovoltaic power plants. IEEE Transactions on Energy Conversion, 34(1), 372-384.

[7] Yu, X., Wang, L., Ma, J., Sun, X., Zhou, X., & Cui, G. (2020). Selectively wetted rigid–flexible coupling polymer electrolyte enabling superior stability and compatibility of high-voltage lithium metal batteries. Advanced Energy Materials, 10(18), 1903939.

[8] Ajoulabadi, A., Ravadanegh, S. N., & Mohammadi-Ivatloo, B. (2020). Flexible scheduling of reconfigurable microgrid-based distribution networks considering demand response program. Energy, 196, 117024.

[9] Gonzalez, D. M., Hachenberger, J., Hinker, J., Rewald, F., Häger, U., Rehtanz, C., & Myrzik, J. (2018, June). Determination of the time-dependent flexibility of active distribution networks to control their TSO-DSO interconnection power flow. In 2018 Power Systems Computation Conference (PSCC) (pp. 1-8). IEEE.

[10] Suarez, F., Parekh, D. P., Ladd, C., Vashaee, D., Dickey, M. D., & Öztürk, M. C. (2017). Flexible thermoelectric generator using bulk legs and liquid metal interconnects for wearable electronics. Applied energy, 202, 736-745.

[11] Impram, S., Nese, S. V., & Oral, B. (2020). Challenges of renewable energy penetration on power system flexibility: A survey. Energy Strategy Reviews, 31, 100539.

[12] Gomis-Bellmunt, O., Sau-Bassols, J., Prieto-Araujo, E., & Cheah-Mane, M. (2019). Flexible converters for meshed HVDC grids: From flexible AC transmission systems (FACTS) to flexible DC grids. IEEE Transactions on Power Delivery, 35(1), 2-15.

[13] Alhurayyis, I., Elkhateb, A., & Morrow, J. (2020). Isolated and nonisolated DC-to-DC converters for medium-voltage DC networks: A review. IEEE Journal of Emerging and Selected Topics in Power Electronics, 9(6), 7486-7500.

[14] Shahzad, S., & Jasińska, E. (2024). Renewable revolution: A review of strategic flexibility in future power systems. Sustainability, 16(13), 5454.

[15] Olivella-Rosell, P., Bullich-Massagué, E., Aragüés-Peñalba, M., Sumper, A., Ottesen, S. Ø., Vidal-Clos, J. A., & Villafáfila-Robles, R. (2018). Optimization problem for meeting distribution system operator requests in local flexibility markets with distributed energy resources. Applied energy, 210, 881-895.

[16] Mohandes, B., El Moursi, M. S., Hatziargyriou, N., & El Khatib, S. (2019). A review of power system flexibility with high penetration of renewables. IEEE Transactions on Power Systems, 34(4), 3140-3155.

[17] Paez, J. D., Frey, D., Maneiro, J., Bacha, S., & Dworakowski, P. (2018). Overview of DC–DC converters dedicated to HVdc grids. IEEE Transactions on Power Delivery, 34(1), 119-128.

[18] An, T., Tang, G., & Wang, W. (2017). Research and application on multi-terminal and DC grids based on VSC-HVDC technology in China. High voltage, 2(1), 1-10.

[19] Maza-Ortega, J. M., Acha, E., García, S., & Gómez-Expósito, A. (2017). Overview of power electronics technology and applications in power generation transmission and distribution. Journal of Modern Power Systems and Clean Energy, 5(4), 499-514.

[20] de Paula García-López, F., Barragán-Villarejo, M., Marano-Marcolini, A., & Maza-Ortega, J. M. (2023). Performance assessment of flexible links in distribution networks using a detailed power losses model. IEEE Open Access Journal of Power and Energy, 10, 550-559.

[21] Degefa, M. Z., Sperstad, I. B., & Sæle, H. (2021). Comprehensive classifications and characterizations of power system flexibility resources. Electric Power Systems Research, 194, 107022.

[22] Papaefthymiou, G., Haesen, E., & Sach, T. (2018). Power System Flexibility Tracker: Indicators to track flexibility progress towards high-RES systems. Renewable energy, 127, 1026-1035.

[23] Zhipeng Jing,Lipo Gao,Yu Mu & Dong Liang. (2024). Flexibility-Constrained Energy Storage System Placement for Flexible Interconnected Distribution Networks. Sustainability(20),9129-9129.

[24] Yunfei Wang,Jiyun Zhao,He Zhang,Hao Wang & Jinxin Wang. (2024). An Output Cooperative Controller for a Hydraulic Support Multi-Cylinder System Based on Neural Network Compensation. Mathematics(12),1866-1866.

[25] Guanpeng Chen,Xue Gao,Yijie Zhao,Xiaojun Xu & Yue Jiang. (2024). Attitude stability control for 6WID unmanned ground vehicle during steering: A collaborative controller considering minimizing tire slip energy loss. Energy131918-.